CrossMark

Electric-Field-Induced Amplitude Tuning of Ferromagnetic Resonance Peak in Nano-granular Film FeCoB-SiO$_2$/PMN-PT Composites

Mei Luo[1,2*], Peiheng Zhou[1,2], Yunfeng Liu[1,2], Xin Wang[1,2] and Jianliang Xie[1,2]

Abstract

One of the challenges in the design of microwave absorbers lies in tunable amplitude of dynamic permeability. In this work, we demonstrate that electric-field-induced magnetoelastic anisotropy in nano-granular film FeCoB-SiO$_2$/PMN-PT (011) composites can be used to tune the amplitude of ferromagnetic resonance peak at room temperature. The FeCoB magnetic particles are separated from each other by SiO$_2$ insulating matrix and present slightly different in-plane anisotropy fields. As a result, multi-resonances appear in the imaginary permeability (μ'') curve and mixed together to form a broadband absorption peak. The amplitude of the resonance peak could be modulated by external electric field from 118 to 266.

Keywords: Magnetoelectric effect, Nano-granular films, Ferromagnetic resonance, Magnetic anisotropy

Background

With the rapid development of electronic industries, the electromagnetic interference problem has become increasingly important and provides challenges for material researchers and radio frequency (RF) design engineers [1]. In order to reduce the undesirable electromagnetic radiation, nano-structural magnetic films have been extensively studied as one of the magnetic shielding materials. Nano-multilayer composites and nanocrystalline films exhibiting large complex permeability (real part μ' and imaginary part μ'' larger than 100) in the gigahertz (GHz) range are reported recently [2, 3]. However, the relatively large complex permittivity (exceeds 10^4) of these kinds of materials is difficult to satisfy the impedance-matching condition in the design method of electromagnetic wave absorption [4]. Magnetic granular films consisting of nanometer-sized ferromagnetic metallic particles (Fe, Co, Ni, and their alloys) randomly distributed in dielectric matrix (SiO$_2$, ZnO, and ZrO$_2$) are developed to solve the above problem [5–8]. These ferromagnetic insulators present high resistivity and hence relatively small permittivity. Nonetheless, the amplitude value of complex permeability cannot be freely tuned in the same sample. This kind of amplitude tuning has important meaning to further implement the active shielding. Therefore, exploiting new frameworks which can present different amplitude value of complex permeability according to the application requirement at room temperature are significant and challenging tasks.

The artificial two-phase systems consisting of ferromagnetic (FM) and ferroelectric (FE) materials have been extensively studied due to attractive potential applications. This heterostructure permits the control of magnetism with the converse magnetoelectric (ME) effect [9, 10]. However, the previous attention on ME effect mainly centered on the study of continuous ferromagnetic films and rarely concerned with ferromagnetic granular films. In this work, ferromagnetic metal-insulator (FeCoB-SiO$_2$) granular film was fabricated on the (011)-oriented 0.71Pb(Mg$_{1/3}$Nb$_{2/3}$)O$_3$-0.29PbTiO$_3$ (PMN-PT) piezoelectric substrate. The amplitude of ferromagnetic resonance peak was tuned from 118 to

* Correspondence: luomeilm@163.com
[1]National Engineering Research Center of Electromagnetic Radiation Control Materials, University of Electronic Science and Technology of China, Chengdu 610054, China
[2]State Key Laboratory of Electronic Thin Films and Integrated Devices, University of Electronic Science and Technology of China, Chengdu 610054, China

Luo et al. Nanoscale Research Letters (2016) 11:493

Page 2 of 5

266 through strong ME coupling at room temperature. This framework provides a simple, active, and efficient way to balance permeability and permittivity of microwave-absorbing films.

Methods

FeCoB-SiO$_2$ granular film was elaborated on the (011)-oriented PMN-PT substrate (10 mm × 5 mm × 0.5 mm) by magnetron co-sputtering system. The radio frequency magnetron sputtering was applied for SiO$_2$ target with a power of 80 W, while DC magnetron sputtering was employed for (Fe$_{65}$Co$_{35}$)$_{90}$B$_{10}$ target with a power of 60 W. Figure 1a shows the schematic illustration of the sputtering system. The working pressure was 0.3 Pa, and the base pressure reached 4×10^{-4} Pa. An external magnetic field (H-field) about 200 Oe was applied along the [100] direction to introduce the in-plane uniaxial magnetic anisotropy in the film. Following the schematic illustration of FeCoB-SiO$_2$/PMN-PT heterostructure shown in Fig. 1b, Au films were deposited on the top of FeCoB-SiO$_2$ granular film and bottom of (011)-oriented PMN-PT substrate as electrodes.
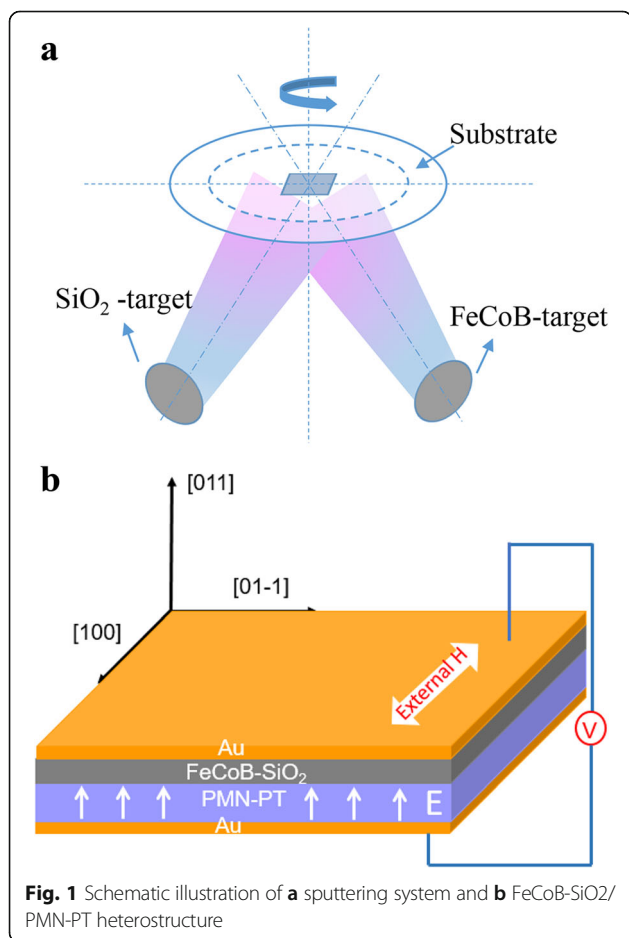
The structure of granular film was investigated by X-ray diffraction (XRD, SHIMADZU XRD-7000) and transmission electron microscopy (TEM, JEM2100F). Hysteresis loops at different electric fields (E-fields) were measured by vibrating sample magnetometer (VSM, RIKEN, JAPAN). The microwave complex permeability was measured by a vector network analyzer (Agilent 8720ET) with the shorted microstrip method without bias H-field. The surface resistivity was measured by four point probe meter (SX1944) at room temperature.

Results and Discussion

The XRD diffraction pattern of FeCoB-SiO$_2$ granular film is shown in Fig. 2a. The FeCoB phase presents polycrystalline structure according to the appearance of (110)$_{FeCo}$ and (200)$_{FeCo}$ diffraction peaks. Diffraction peaks of SiO$_2$ phase are not observed, which indicates
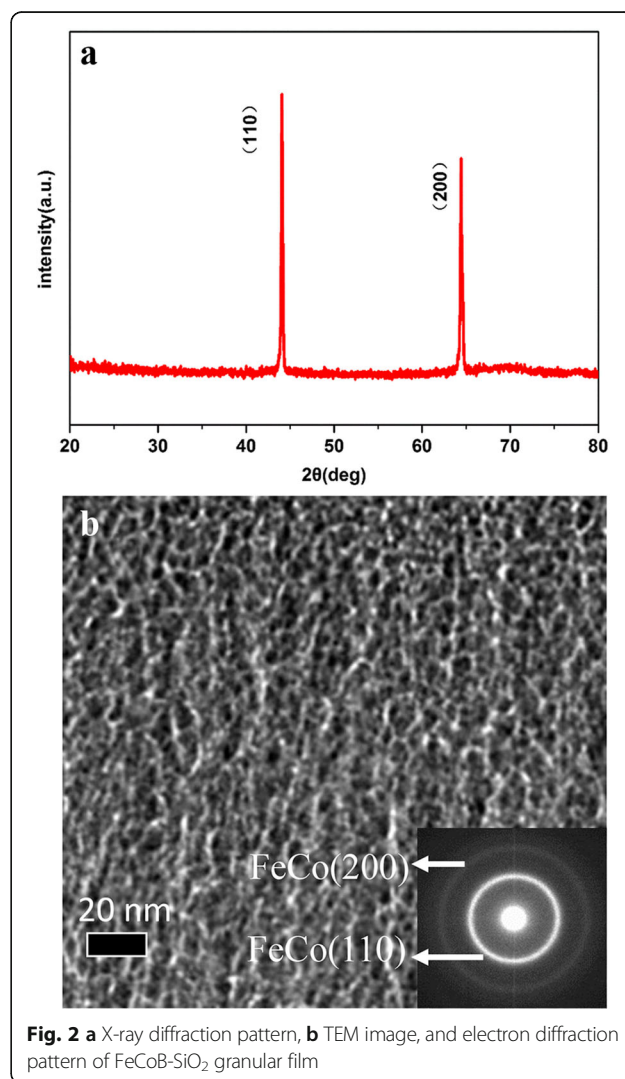

Fig. 1 Schematic illustration of **a** sputtering system and **b** FeCoB-SiO2/PMN-PT heterostructure

Fig. 2 a X-ray diffraction pattern, **b** TEM image, and electron diffraction pattern of FeCoB-SiO$_2$ granular film

Luo *et al. Nanoscale Research Letters* (2016) 11:493

Page 3 of 5

that the SiO_2 is an amorphous phase. Figure 2b shows the TEM image and electron diffraction pattern of the FeCoB-SiO_2 granular film. It is found that SiO_2 phase (shows in bright contrast) wraps around the FeCoB alloy particles (show in dark contrast) and hence forms the insulating network matrix. The FeCoB particles have a non-uniform size distribution from 2 to 10 nm in diameter, and the distance between them are about 2 nm. The electron diffraction pattern from (110) and (200) planes indicates FeCoB particles are polycrystalline structure, which is consistent with the result of XRD measurement. The surface resistivity ρ of FeCoB-SiO_2 granular film is 8550 $\mu\Omega$ cm, which is bigger than continuous FeCoB films (ρ is often given as close to zero).

Figure 3 shows the external E-field dependence of magnetic hysteresis loops of FeCoB-SiO_2/PMN-PT composite. As can be seen from Fig. 3a, FeCoB-SiO_2 granular film exhibits obvious in-plane uniaxial magnetic anisotropy with E-field of 0 kV/cm, where the curve obtained along the [01-1] direction shows hard axis behavior and the [100] direction shows easy axis behavior. When the E-field is applied through the thickness direction of PMN-PT substrate, the remanent magnetization of FeCoB-SiO_2 granular film decreases along [100] direction and increase along [01-1] direction. This result implies a strong strain-driven ME coupling between FeCoB particles and PMN-PT substrate and a fundamental change of the magnetic anisotropy field in FeCoB-

SiO_2 granular film. A large E-field-induced magnetoelastic effective field (H_{eff}) is expressed as [11]

$$H_{eff} = 3\lambda Y dE/M_s, \qquad (1)$$

where d is the piezoelectric coefficient, λ is the magnetostriction constant, and M_s is the saturation magnetization. The H_{eff} coming from the ME coupling not only affects the static magnetic properties of FeCoB-SiO_2 granular film but also affects the dynamic magnetic properties.

The complex permeability curves of the FeCoB-SiO_2/PMN-PT composite under different E-fields across the thickness of the PMN-PT are shown in Fig. 4. For FeCoB-SiO_2 granular film, it is considered that almost all the magnetic particles are separated from each other by non-magnetism phase because the FeCoB particles are embedded in SiO_2 matrices as shown in Fig. 2b. Since the size of the magnetic particles is smaller than the critical value of single domain which is dozens of nanometers for $Fe_{65}Co_{35}$, FeCoB particles can be characterized by a single domain spontaneous state [12]. The ferromagnetic exchange interaction forces the magnetic moments to align parallel and deviates from the easy axis of each individual FeCoB particle. As a consequence, the local anisotropies of FeCoB-SiO_2 granular film are average out according to the random anisotropy theory proposed by Herzer [13]. Thus, magnetic moment orientations of each single domain are along their
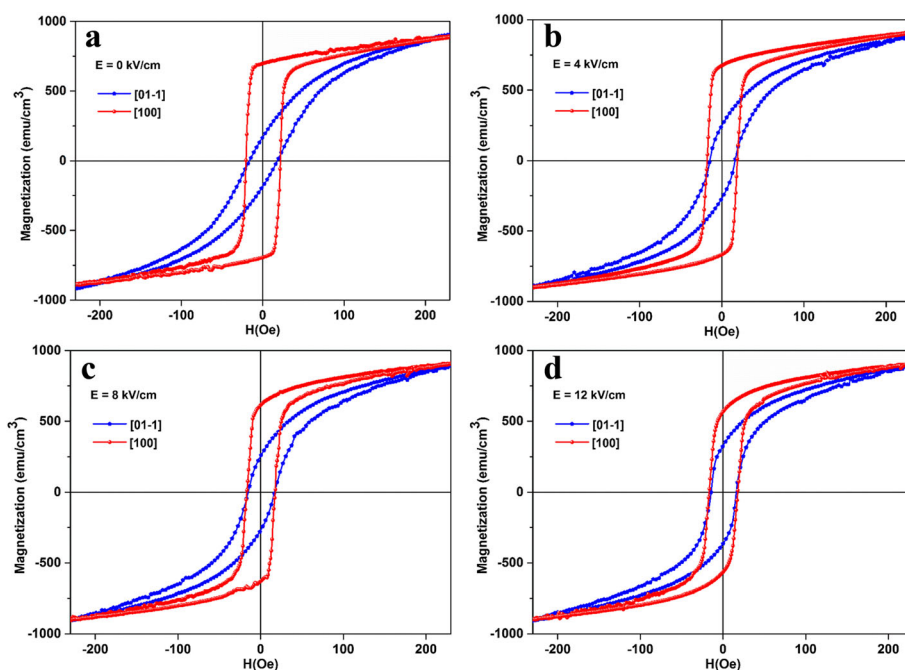

Fig. 3 In-plane hysteresis loops of FeCoB-SiO_2/PMN-PT at **a** 0 kV/cm, **b** 4 kV/cm, **c** 8 kV/cm, and **d** 12 kV/cm

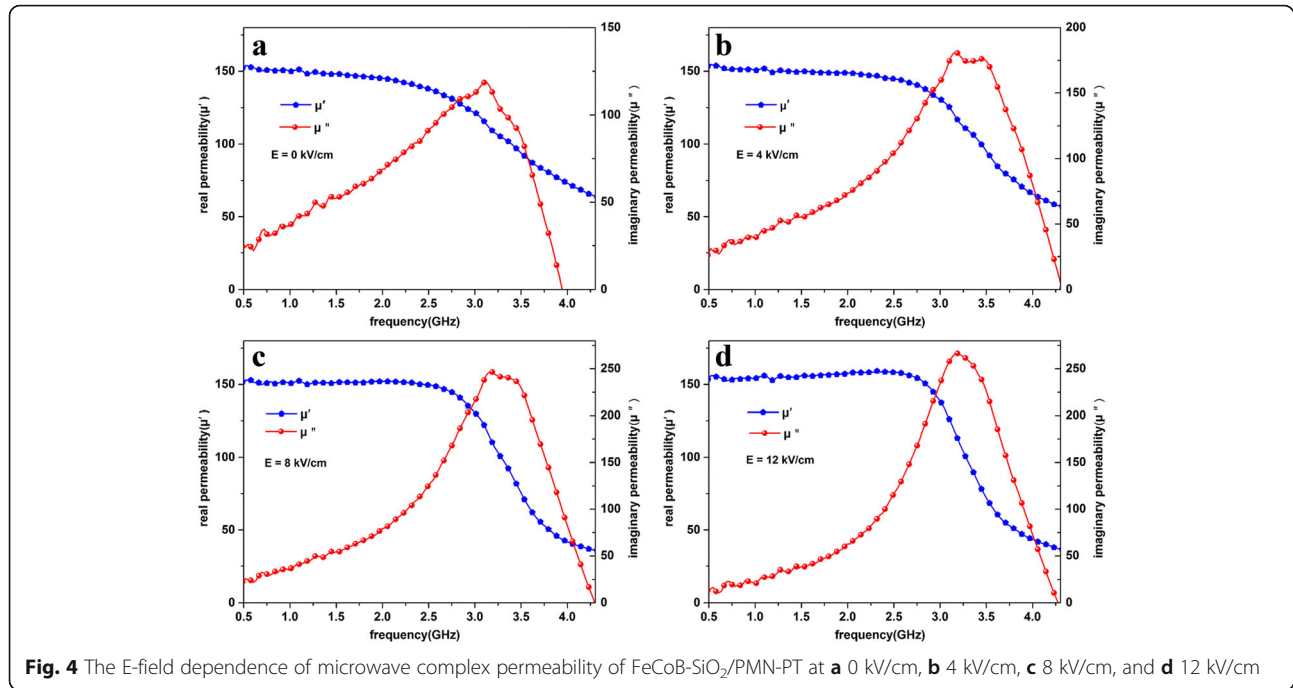Luo *et al. Nanoscale Research Letters* (2016) 11:493

Page 4 of 5

Fig. 4 The E-field dependence of microwave complex permeability of FeCoB-SiO$_2$/PMN-PT at **a** 0 kV/cm, **b** 4 kV/cm, **c** 8 kV/cm, and **d** 12 kV/cm

respective preferred direction of magnetization and disordered in plane. In the meantime, the magnetic moments of interfacial atoms of magnetic particles are influenced by the pinning effect of the SiO$_2$ on the interface. Each particle undergoes totally different pinning process due to the different shapes and sizes. Together with the abovementioned effects, it is considered that the in-plane anisotropy fields of each FeCoB particle are slightly different. These minor differences would not show up explicitly in static magnetic hysteresis loop, but implicitly as part of dynamic permeability spectra. As Fig. 4a shows, real permeability (μ') curve exhibits slight step, which is similar to FeCoB/SiO$_2$/FeCoSiB magnetic films. Owing to the differences between FeCoB and FeCoSiB magnetic properties, two resonance peaks of the complex permeability spectra are observed in [3]. In our case, the multiple magnetic states also result in multi-resonance phenomenon and broaden the resonance band by mixing all the resonance bands together. When the E-field is applied, the E-field-induced in-plane effective anisotropic field (H_{eff}) influences the shift of ferromagnetic resonance frequency (f_r) by the Kittel equation [14]

$$f_r = \gamma \sqrt{(H_r + H_{eff})(H_r + H_{eff} + 4\pi M_s)}, \qquad (2)$$

where γ is the gyromagnetic ratio. Based on the E-field dependence of static magnetic hysteresis loops, the total in-plane anisotropic fields of FeCoB-SiO$_2$ granular film are decreased with E-field. The H_{eff} brings negative effect to total in-plane anisotropic fields. As a matter of

fact, the strain responses of PMN-PT substrate under the converse piezoelectric effect are not homogeneous in plane [15]. This is negligible for continuous ferromagnetic films, but important for granular films. The strain of piezoelectric substrate reduces gradually from edge to center. When the E-field is 4 kV/cm, magnetic properties of nanoparticles which are located at the edge of substrate are effectively changed by H_{eff}, while nanoparticles located at the center of substrate are basically unchanged. Hence, a part of ferromagnetic resonance peaks moves to low frequencies and mixes with those unchanged peaks located at low frequencies. Because of the additive effect of multiple ferromagnetic resonance peak, the amplitude of the peak has got an improvement. Along with the gradually increasing of E-field, magnetoelastic H_{eff} increases and affects more FeCoB particles. The amplitude of the ferromagnetic resonance peak is further increased due to the more peaks shift to low frequency and mix. We can see that multiple peak mixes into single peak and the amplitude of the resonance peak changes dramatically with E-fields, being 118 at 0 kV/cm, 181 at 4 kV/cm, 246 at 8 kV/cm, and 266 at 12 kV/cm, respectively. This framework realizes the tuning of amplitude value of the imaginary part μ'' by E-fields in a certain frequency range.

Conclusions
In summary, we have fabricated a heterostructure of FeCoB-SiO$_2$/PMN-PT (011) and studied the ME effect by E-field-induced amplitude tuning of ferromagnetic resonance peak in GHz range. Almost all the FeCoB

Luo *et al. Nanoscale Research Letters* (2016) 11:493

Page 5 of 5

magnetic particles are separated from each other by non-magnetism phase SiO_2 and the slightly different in the in-plane anisotropy fields. As a result, the imaginary permeability (μ'') curve presents broad-bandwidth and multi-peak resonance. The multiple resonant peaks mix into a single peak, and the amplitude of the resonance peak changes from 118 to 266 with increasing E-field. This framework provides an important opportunity for balancing permeability and permittivity of microwave absorbers.

Abbreviations
E-field: Electric field; FE: Ferroelectric; FM: Ferromagnetic; H_{eff}: Magnetoelastic effective field; ME: Magnetoelectric; PMN-PT: $0.71Pb(Mg_{1/3}Nb_{2/3})O_3$-$0.29PbTiO_3$; RF: Radio frequency; TEM: Transmission electron microscopy; VSM: Vibrating sample magnetometer; XRD: X-ray diffraction

Authors' Contributions
ML carried out the study of the $FeCoB-SiO_2/PMN-PT$ composites and draft the manuscript. YL measured the composites and statistical analysis. PZ and XW carried out the data integration and manuscript modification. JX conceived of this study and design composites. All authors read and approved the final manuscript.

Competing Interests
The authors declare that they have no competing interests.

References
1. Wu X, Yan S, Liu W, Feng Z, Chen Y, Harris VG (2016) Influence of particle size on the magnetic spectrum of NiCuZn ferrites for electromagnetic shielding applications. J Magn Magn Mater 401:1093–1096
2. Yang FF, Yan SS, Yu MX, Dai YY, Kang SS, Chen YX, Pan SB, Zhang JL, Bai HL, Xu TS (2012) High-frequency electromagnetic properties of compositionally graded FeCoB-SiO2 granular films deposited on flexible substrates. J Appl Phys 111:113909–113904.
3. Zhang L, Zheng H, Zhu W, Li M, Zhang M, Wang N, Lu H, Xie J, Deng L (2016) Study of magnetic properties and double resonance peaks of FeCoB/SiO2/FeCoSiB magnetic films. J Alloys Compd 657:174–178
4. Deng L, Feng Z, Jiang J, He H (2007) Percolation and microwave characteristics of CoFeB–SiO2 nano-granular films. J Magn Magn Mater 309:285–289
5. Yang FF, Yan SS, Yu MX, Kang SS, Dai YY, Chen YX, Pan SB, Zhang JL, Bai HL, Zhu DP (2013) Soft magnetic and high-frequency properties of FeCoB–SiO2 granular films deposited on flexible substrates. J Alloys Compd 558:91–94
6. Yang Y, Zhong L, Lan W, Bi X, Yang Y, Zhong L, Lan W, Bi X (2011) Microstructure and magnetic behaviors of FeSi-ZrO2 nanocomposite films. Rare Met 30:533–537
7. Wang G, Zhang F, Zuo H, Yu Z, Ge S (2010) Fabrication and Magnetic Properties of Fe65Co35–ZnO Nano-Granular Films. Nanoscale Res Lett 5:1107–1110
8. Iqbal J, Jan T, Yu R, Naqvi SJH, Ahmad I (2014) Doping Induced Tailoring in the Morphology, Band-Gap and Ferromagnetic Properties of Biocompatible ZnO Nanowires, Nanorods and Nanoparticles. Micro Nano Lett 6:242–251
9. Liu M, Hoffman J, Wang J, Zhang J, Nelson-Cheeseman B, Bhattacharya A (2013) Non-volatile ferroelastic switching of the Verwey transition and resistivity of epitaxial Fe3O4/PMN-PT (011). Sci Rep 3:1876
10. Zhou Z, Zhao S, Gao Y, Wang X, Nan T, Sun NX, Yang X, Liu M (2016) The memory effect of magnetoelectric coupling in FeGaB/NiTi/PMN-PT multiferroic heterostructure. Sci Rep 6:20450
11. Lou J, Reed D, Pettiford C, Liu M, Han P, Dong S, Sun NX (2008) Giant microwave tunability in FeGaB/lead magnesium niobate-lead titanate multiferroic composites. Appl Phys Lett 92:262502–262503
12. Li Z, Qin S, Xing W, Xie J, Deng L (2013) Effect of multilayer structure on high-frequency properties of FeCo/(FeCo)0.63(SiO2)0.37 nanogranular films on flexible substrates. Nanoscale Res Lett 8:1–4
13. Herzer G (1990) Grain size dependence of coercivity and permeability in nanocrystalline ferromagnets. IEEE Trans Magn 26:1397–1402
14. Liu M, Howe BM, Grazulis L, Mahalingam K, Nan T, Sun NX, Brown GJ (2013) Voltage-Impulse-Induced Non-Volatile Ferroelastic Switching of Ferromagnetic Resonance for Reconfigurable Magnetoelectric Microwave Devices. Adv Mater 25:4886–4892
15. Andersen T, Andersen MA, Thomsen OC (2012) Simulation of Piezoelectric Transformers with COMSOL. COMSOL conference